Insulin crystallization: The route from hanging-drop vapour diffusion to controlled crystallization in droplet microfluidics

Joana Ferreira,[1,2†] Zsuzsa Sárkány,[3] Filipa Castro,[2] Fernando Rocha,[2] and Simon Kuhn[1*]*

[1] KU Leuven, Department of Chemical Engineering, Celestijnenlaan 200F, 3001 Leuven, Belgium

[2] LEPABE – Laboratory for Process Engineering, Biotechnology and Energy, Faculty of Engineering, University of Porto, Rua Dr. Roberto Frias, 4200-465 Porto, Portugal

[3]IBMC – Instituto de Biologia Molecular e Celular, University of Porto, Rua Alfredo Allen, 4200-135 Porto, Portugal

Abstract

Although half a century has passed since the mapping of the insulin structure, this globular protein is still currently being investigated. Crystalline drug formulations might replace the subcutaneous injections for diabetes treatment. However, these crystalline forms require carefully tailored properties to sustain controlled release (*e.g.* longer storage lifetimes and higher purity). Among others, crystal size polydispersity might reduce the speed of insulin release. Here, two distinct crystallization techniques are applied to study insulin crystallization, hanging-drop vapour diffusion and microbatch (droplet microfluidics), and an operating regime map is derived. Rhombohedral insulin

crystals with variable size are produced inside the microdroplets for a broad range of insulin concentrations, while aggregate and/or agglomerate formation is observed during the hanging-drop experiments at low protein concentrations. These differences are likely explained by the way acetone evaporation is controlled in each technique. In fact, circular dichroism spectra reveal differences on insulin's secondary structure at variable acetone concentration, including the reduction of α-helical content, with no visible β-sheet-rich structures or random coils. Finally, contrary to what has been reported for other proteins, no temperature effect on insulin crystal size is observed within a range from 10 °C to 20 °C. This work highlights the formation of insulin crystals in confined microdroplets towards a better control over the insulin crystal size.

1. Introduction

Dorothy Crowfoot Hodgkin contributed enormously to the field of biological macromolecules [1]. Among Hodgkin's longest-lasting accomplishments is the mapping of the insulin structure, which involved 35 years of work. Although the study was concluded in 1969, the importance of this polypeptide hormone for diabetes treatment is still a up-to-date concern [2]. Overall, the deficiency or resistance to insulin causes profound deregulation of metabolic processes (*i.e.* control of blood glucose) [3] resulting in disorders such as diabetes mellitus and obesity [4]. Over the last 50 years, there has been an increasing focus on long-acting crystalline drug formulations [5] to replace frequent subcutaneous injections by increasing dose efficacy and patient compliance [6].

Insulin is the only protein produced in a healthy human body in crystalline form, and this fact highlights the relevance of crystallization studies [7]. Crystalline forms with

carefully tailored properties often have longer storage lifetimes and higher purity than the dissolved forms [8]. The type, size and morphology of the crystals affect the insulin release rate. The slow dissolution rate of protein crystals allows sustained drug release [5], where narrow crystal size distribution (CSD) and shape uniformity are required [4]. This might be achieved by several nucleation events taking place at the same time [9]. Throughout the years, multiple research groups from biochemistry to engineering tried to crystallize insulin under different operating conditions (*e.g.* crystallizing agent and buffer solutions, pH, among others).

After the first successful isolation of an insulin crystal reported by Abel (1926) [10], Schlichtkrull [11–15] published a series of articles describing different methodologies to crystallize insulin. These initial studies were followed by the works of Kadima *et al.* (1991) [16], Yip & Ward (1996) [17], Nettleton *et al.* (2000) [18], Mühlig *et al.* (2001) [19], Bromberg *et al.* (2005) [20], Govardhan *et al.* (2005) [21], Norrman & Schlukebier (2007) [6], Pease *et al.* (2010) [22], Chatani *et al.* (2015) [23], Fili *et al.* (2015) [24], and Dolui *et al.* (2018) [25]. Additionally, Barlow (2017) [26] and Alexandrov & Nizovtseva (2019) [27] based on the experimental data from Schlichtkrull [11–15] developed insulin crystallization kinetic models to predict *e.g.* kinetics of supersaturation decay, homogeneous nucleation rate, and CSD. Furthermore, with the experimental protocol developed by Bergeron *et al.* (2003) [3], several works have emerged using similar crystallization conditions [7,9,28–30], and an overview of the optimized crystallization conditions can be found in Dimitrov *et al.* (2013) [31] and Hodzhaoglu *et al.* (2016) [32]. Within the broad range of crystallization techniques, Maeda *et al.* (2004) [33] performed dialysis experiments, while Parambil *et al.* (2011) [34] crystallized using oscillatory flow in capillaries. More recently, Chen *et al.* (2017) [35] and Li *et al.* (2019) [36] reported single-nucleation

events in micro- and nanodroplets, respectively; and Contreras-Montoya *et al*. (2021) [37] developed composite crystal formulation by crystallizing insulin in agarose and hydrogels.

A complementary analysis to the crystallization process involves a better understanding of protein structural transformations and/or folding pathways. Techniques such as X-ray diffraction [25,38,39], FTIR (Fourier transform infrared spectroscopy) [18,23,38], AFM (atomic force microscopy) [17,22,25,40,41], CD (circular dichroism) [22,25,38–52], among others [18,22,23,25,38,40,41,46–48] have been used to obtain structural insights in solution. Insulin crystallizes as a hexamer, while in solution occurs as an equilibrium mixture of monomers, dimers, tetramers, hexamers, and possibly higher associated states [51]. Insulin molecules tend to form dimers (as in the presence of hydrochloric acid [40,46]), and hexamers in the presence of metallic ions (*e.g*. Zn^{2+}) [24,48].

In this work, insulin crystallization experiments are performed in vapour diffusion microwells and in a microfluidic reactor. Firstly, the range of crystallization conditions is explored through hanging-drop experimentation (microwells). Secondly, to gain control over the insulin crystallization process and thus to ensure a uniform CSD, microbatch assays are conducted. The microfluidic microreactor with an integrated temperature control is capable to produce uniform and stable confined microdroplets [53,54]. To the best of our knowledge, despite all the efforts from the scientific community to produce insulin crystals, this study constitutes the first attempt towards insulin crystallization trials in multiphase microsystems, where the lowest crystallization volume is reported. Due to the reduced crystallization volumes, the present study intends to highlight a more rational

approach to crystallize insulin through the control of operating variables promoting protein structure conformations in solution that are more favourable to crystallization.

2. Methodology and Materials

2.1. Crystallization solution preparation

Recombinant human insulin (Sigma-Aldrich, 5.808,00 $g \cdot mol^{-1}$, CAS-No. 11061-68-0) was used in the experiments without further purification. The protocol proposed by Bergeron *et al*. (2003) [3] was followed and optimized. The crystallization solution composition included 20 mM hydrochloric acid (HCl, solvent) (Chem-Lab Analytical, CAS-No. 7647-01-0), 100 mM zinc chloride, anhydrous power ($ZnCl_2$, precipitating agent) (Sigma-Aldrich, CAS-No. 7646-85-7), 200 mM trisodium citrate, dihydrate (TC, buffer) (Sigma-Aldrich, CAS-No. 6132-04-3), and 20% (v/v) neat acetone (co-solvent) (VWR International, CAS-No. 67-64-1). Ultrapure water (Milli-Q water, resistivity of 18.3 $M\Omega \cdot cm^{-1}$ at 20 ºC) was utilized.

Initially, insulin was dissolved in highly diluted HCl at different concentrations ranging from 2.5 $mg \cdot ml^{-1}$ to 15 $mg \cdot ml^{-1}$. Afterwards, $ZnCl_2$, TC, and acetone were consecutively added. Thus, the final concentrations of the components in solution were: 6.25 mM $ZnCl_2$, 62.5 mM TC, and 12.5% (v/v) acetone. The stock solutions were prepared at room temperature without any pre-heating or centrifugation steps. All solutions were filtered using syringe filters (Puradisc FP 30 mm, cellulose acetate, 0.2 μm) (Sigma-Aldrich, Whatman) to remove large aggregates [19].

2.2. Screening of insulin crystallization conditions

The hanging-drop vapour diffusion technique was used to screen the crystallization conditions. Preliminary insulin crystallization trials were carried out using 24-well VDX plates (Hampton Research) and 22 mm siliconized coverslips (Hampton Research) sealed with high vacuum grease (Dow Corning). Each drop (8 μl) was composed by a mixture of insulin and reservoir ($ZnCl_2$, TC, acetone) solutions. The drop was placed in equilibrium with the reservoir (1 ml) solution. The reservoir concentration was kept constant, while the ratio between the protein and reservoir concentrations in the drop was varied.

Insulin crystallization assays were either conducted at room temperature or at 4 ºC using an incubator (PHCbi, MIR-254). The crystallization plates were analysed using a microscope (Nikon SMZ-25), equipped with a Nikon DS-Fi3 digital camera, where time-lapse picture capturing, and video recording was performed. The crystallization plates were periodically checked for the presence of crystals and their size. This analysis was conducted using *NIS-Elements Advanced Research* [55]. The success of a crystallization experiment was defined by the fraction between the drops with crystals and the total number of drops, where a value of 75% corresponded to a successful crystallization assay.

2.3. Microfluidic experiments

The experimental set-up (Figure 1) and methodology used to perform crystallization trials in a droplet-based microreactor were described in Ferreira *et al*. (2018) [56] and Ferreira *et al*. (2020) [57]. The droplet-based microfluidic platform was capable to produce uniform and stable droplets with a large flexibility in terms of droplet volume (0.9 – 18 μL) [56].

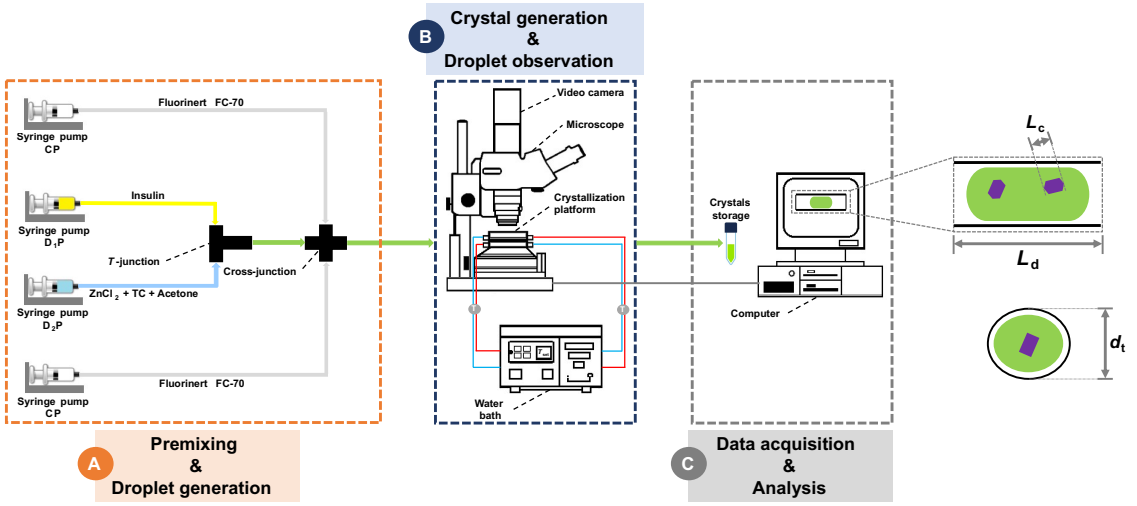

Figure 1. Schematic overview of the experimental set-up: **(A)** Injection of the fluid phases using syringe pumps [CP (continuous phase) – Fluorinert FC-70; DP (dispersed phase) – 1. Insulin solution, 2. Precipitant solution – Precipitating agent ($ZnCl_2$) + buffer (TC) + co-solvent (acetone)]. **(B)** Microfluidic platform with integrated temperature control. Optical microscopy is used to monitor the experiments, where the crystals are collected at the end of the platform. **(C)** Crystal(s) counting and droplet length and crystal size measurements by image analysis techniques. [L_d defines the droplet length (1 mm), L_c the crystal size, d_t the microchannel diameter (1 mm)].

The flow rates of the continuous [Fluorinert™ FC-70 (Sigma-Aldrich, CAS No. 338-84-1)] and dispersed (crystallization solutions premixed before the addition of the carrier fluid) phases were equal to 1.0 ml·min^{-1} and 0.5 ml·min^{-1}, respectively. These flow rates were kept constant, except for the ratio between the protein (insulin) and crystallization ($ZnCl_2$, TC, and acetone) solutions, but always maintaining the total flow rate of the dispersed phase. In this flow-focusing geometry [Figure 1-(A)], the squeezing flow regime corresponds to Capillary (Ca) numbers in the following ranges: $Ca_c < 10^{-1}$ and $Ca_d < 10^{-2}$ [58], which covers the Capillary numbers of the hydrodynamic condition studied in this work ($Ca_c = 1.7 \times 10^{-2}$ and $Ca_d = 2.6 \times 10^{-4}$). Therefore, the microbatch crystallization assays were conducted in microdroplets with a fixed volume of 1 μl (droplet length of 1 mm) generated in a microchannel with a diameter of 1 mm. Lastly, the initial insulin concentrations were 2.5, 5.0 and 15.0 mg·ml^{-1}.

During these experiments, the insulin crystal size in confined microdroplets was measured. Typically, the size of a rhombohedral insulin crystal was defined as the greatest diagonal of the crystal [12,35]. On average, 150 droplets were analysed and, at least, 500 crystals measured per experiment. The analysis was conducted using *NIS-Elements Advanced Research* [55] and *ImageJ software* [59].

2.4. Circular dichroism (CD) spectroscopy

Insulin solutions are diluted to a concentration of 20 μM and 200 μM. Far- and near-UV circular dichroism measurements were analysed in the wavelength range of 260 nm to 190 nm and 350 nm to 260 nm, respectively using a J815 circular dichroism spectrometer (JASCO) at 20 ºC in a quartz cuvette with 1 cm pathlength.

3. Results and Discussion

3.1. Hanging-drop vapour diffusion experiments

The screening of crystallization conditions was carried out by hanging-drop vapour diffusion assays. As suggested by Bergeron *et al*. (2003) [3], the first crystallization trials were conducted at 4 °C with an initial insulin concentration of 15 mg·ml^{-1}. The main findings resulting from the initial screening of crystallization conditions are displayed in Figures 2–5. Additional results at lower protein concentrations are shown in *SI – S1. Screening of insulin crystallization conditions*.

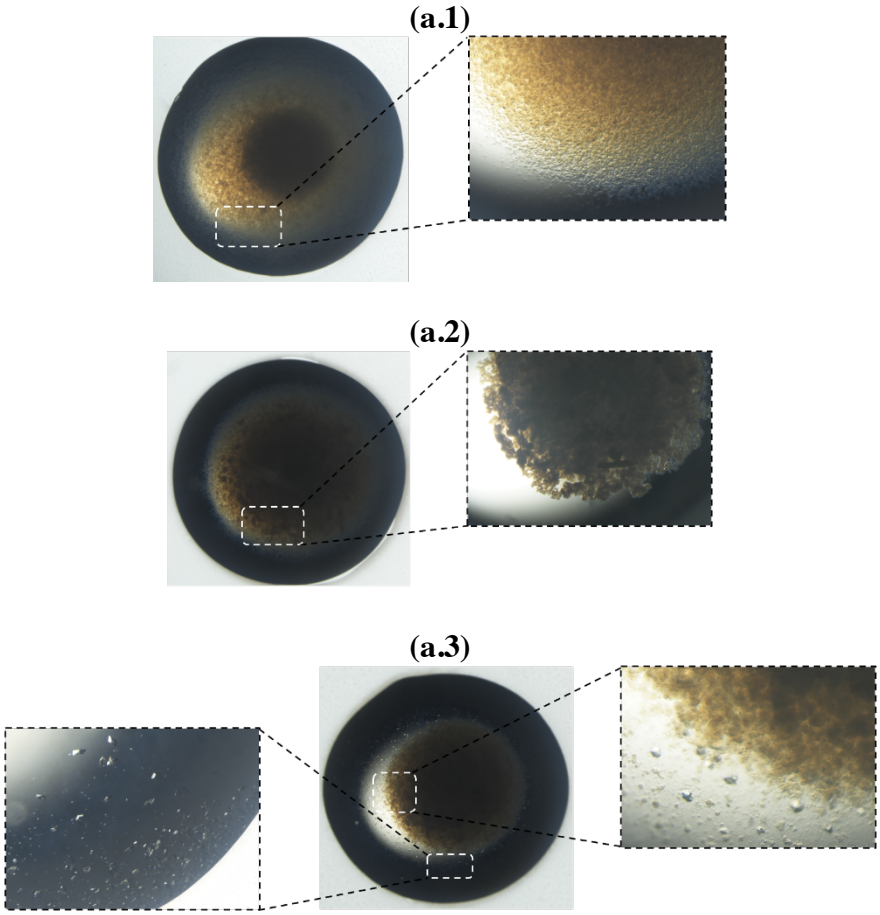

Figure 2. Hanging-drop crystallization for insulin and precipitating agent ($ZnCl_2$) solution concentrations of 7.5 $mg \cdot ml^{-1}$ and 3.1 mM, respectively after 1 day at 4 °C: **(a.1)** to **(a.3)** represent different drops and close-ups.

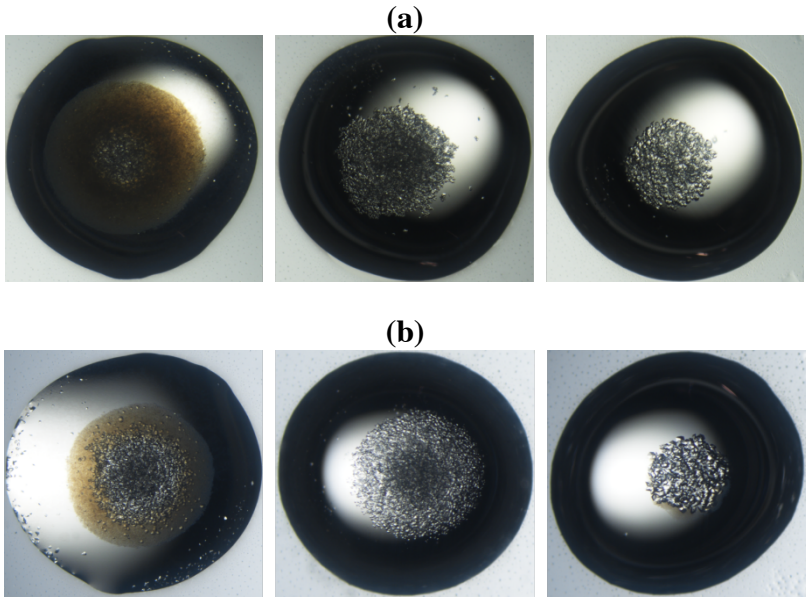

Figure 3. Hanging-drop crystallization for insulin and precipitating agent ($ZnCl_2$) solution concentrations of 7.5 $mg \cdot ml^{-1}$ and 3.1 mM, respectively after: **(a)** 5 days and **(b)** 15 days at 4 °C for different drops.

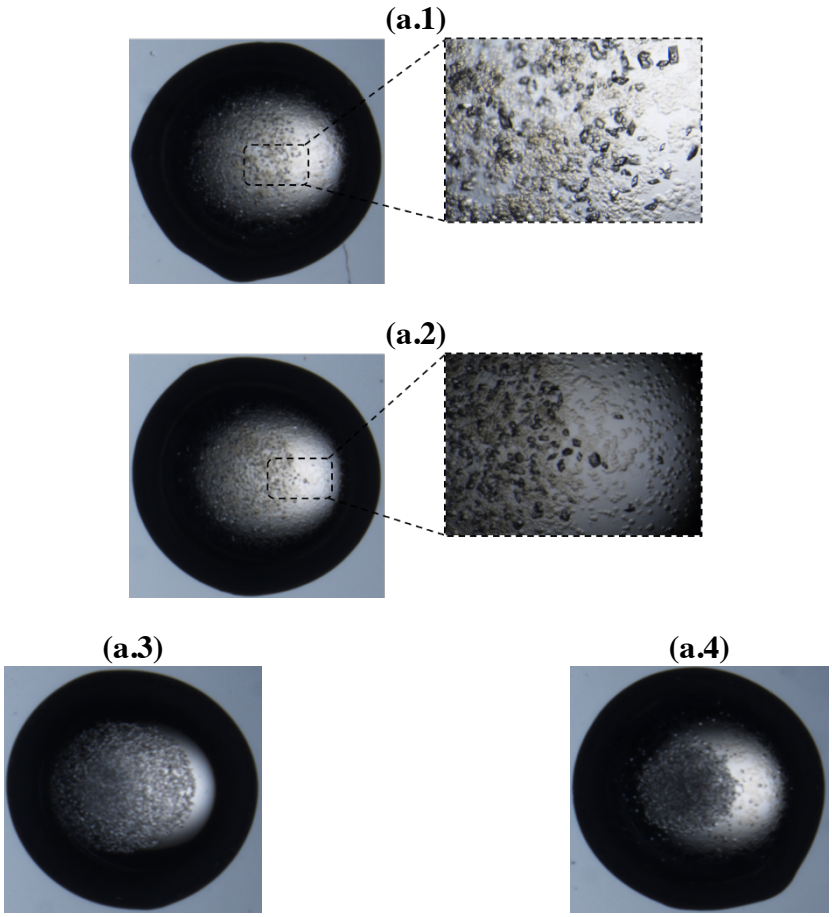

Figure 4. Hanging-drop crystallization for insulin and precipitating agent ($ZnCl_2$) solution concentrations of 5 $mg \cdot ml^{-1}$ and 4.2 mM, respectively after 4 h at 4 °C: **(a.1)** to **(a.4)** represent different drops and close-ups.

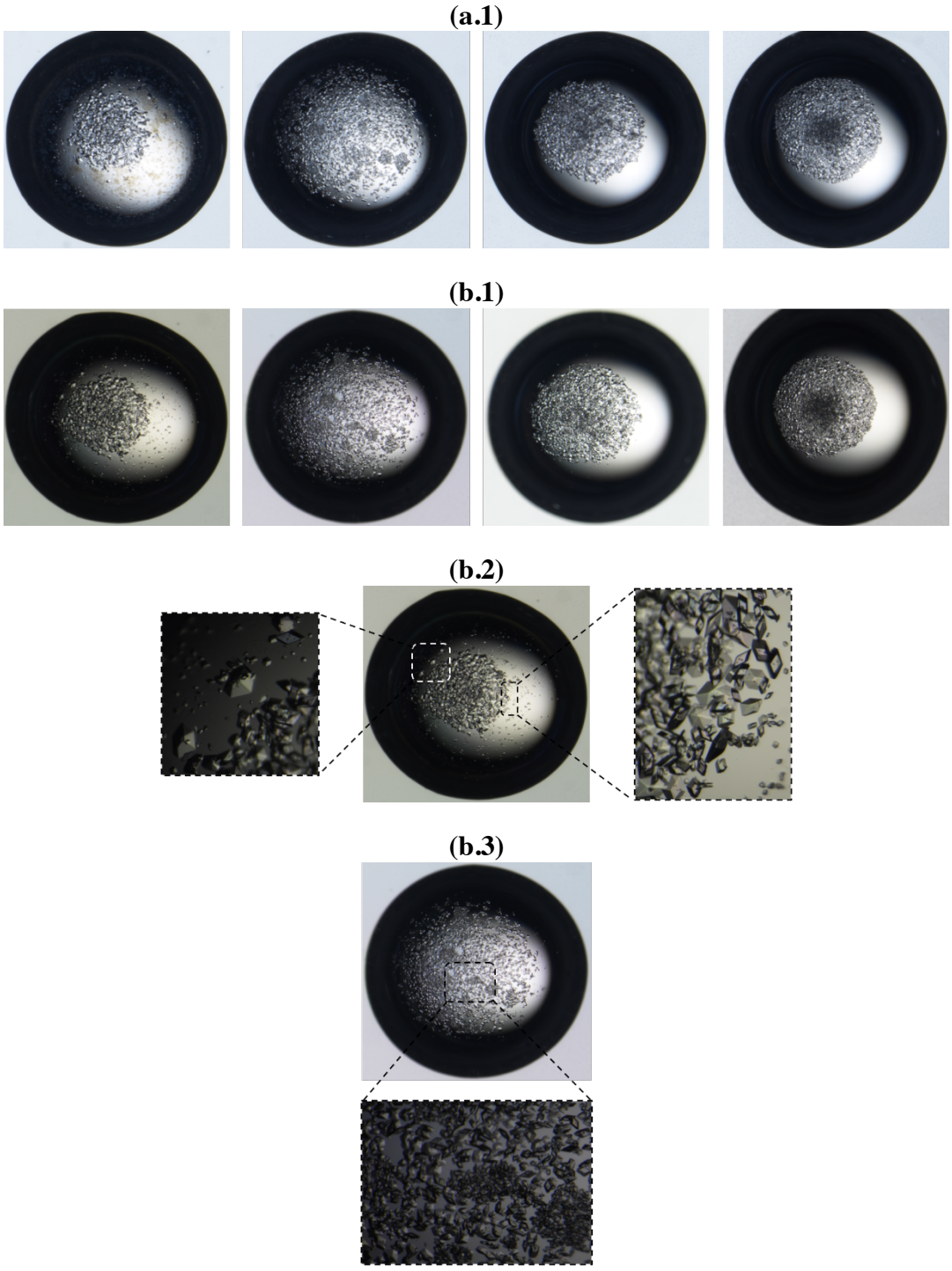

Figure 5. Hanging-drop crystallization for insulin and precipitating agent ($ZnCl_2$) solution concentrations of 5 $mg \cdot ml^{-1}$ and 4.2 mM, respectively after **(a)** 5 days, and **(b)** 15 days at 4 °C: **(1)** Different drops, and **(2)** and **(3)** close-ups.

The results demonstrate the crucial contribution of insulin concentration in solution to the formation of insulin aggregates and/or agglomerates (Figures 2–5). It appears that a lower insulin concentration leads to a suppression of insulin aggregates

and/or agglomerates (Figures 4 and 5). However, for the studied range of insulin concentration, the disappearance of insulin aggregates and/or agglomerates takes a distinct time interval. Hardly any aggregates and/or agglomerates are observed after 5 days at low insulin concentration (Figure 5, insulin concentration of 5 $mg \cdot ml^{-1}$), while their presence is still verified after 15 days at high insulin concentration (Figure 3, insulin concentration of 7.5 $mg \cdot ml^{-1}$). Afterwards, insulin rhombohedral crystals start to appear in the bulk phase. Although crystal formation is observed, excessive nucleation takes place, which results in the formation of many crystals with a broad size range (Figures 3 and 5).

Due to very slow transport mechanisms (diffusion and convection) within the hanging-drop, after combining the drops of insulin and reservoir solutions, the final drop is slightly turbid (Figure 4). Solution turbidity, possibly related to precipitation events [19], tends to disappear over time, which might indicate that the aggregates and/or agglomerates are consumed (Figure 5) [60]. Mühlig *et al*. (2001) [19] reported the occurrence of precipitation after the buffer (sodium citrate) addition, which resulted in a cloudy solution at higher supersaturation ratios [19]. Chen *et al*. (2017) [35] and Hodzhaoglu *et al*. (2016) [32] highlighted the importance of co-solvents (*e.g*. acetone, phenol, among others) to obtain well-formed insulin crystals without faces defects.

3.2. Droplet microfluidics (microbatch) experiments

After the screening of crystallization conditions by hanging-drop vapour diffusion, insulin crystallization experiments were performed in a droplet-based microfluidic device for an extended range of insulin and precipitating agent ($ZnCl_2$) solution concentrations. The main results are presented in Figures 6 and 7.

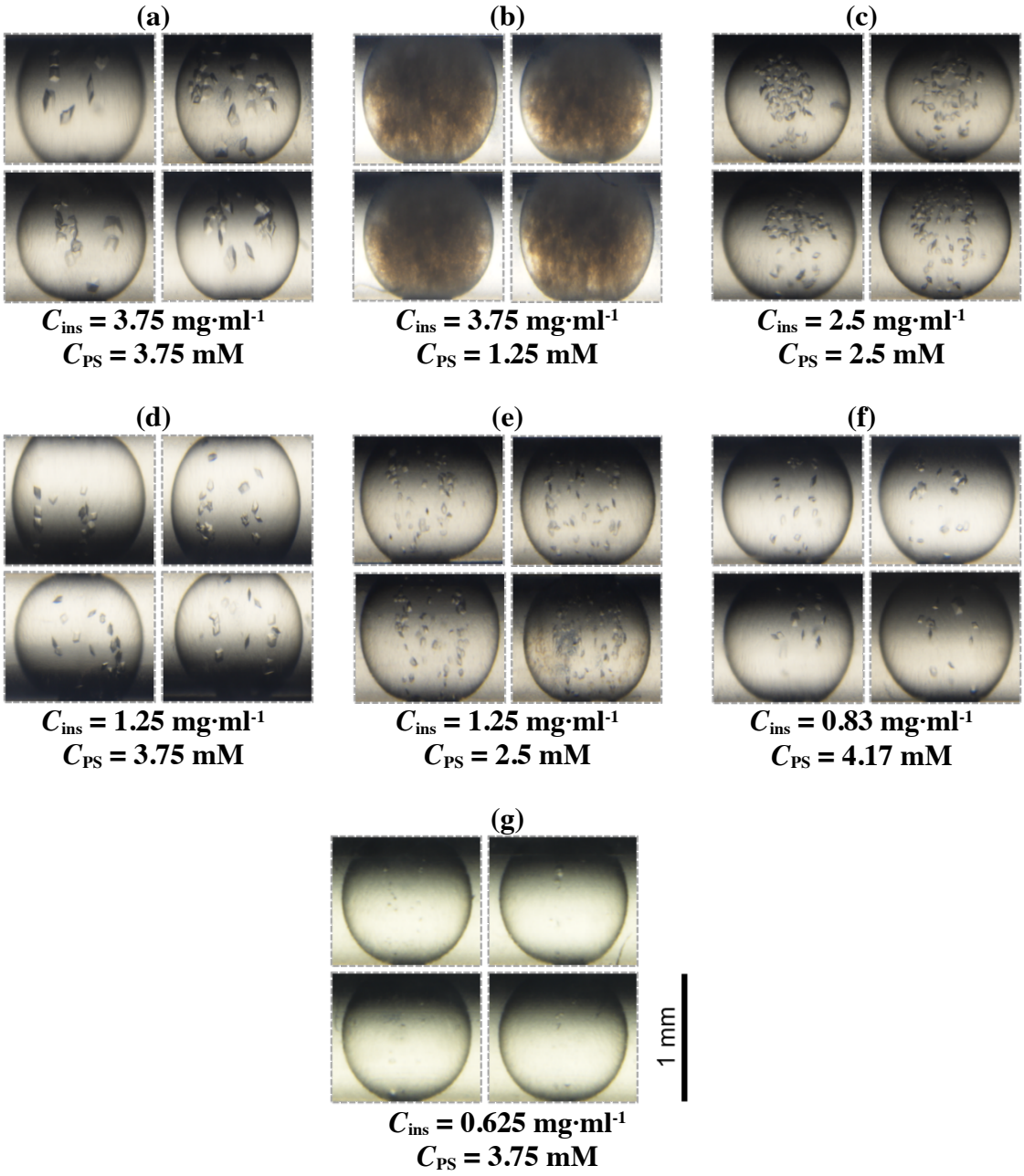

Figure 6. Insulin crystallization in microdroplets for variable insulin (C_{ins}) and precipitating agent ($ZnCl_2$) (C_{PS}) concentrations at 20 ºC after 1 day.

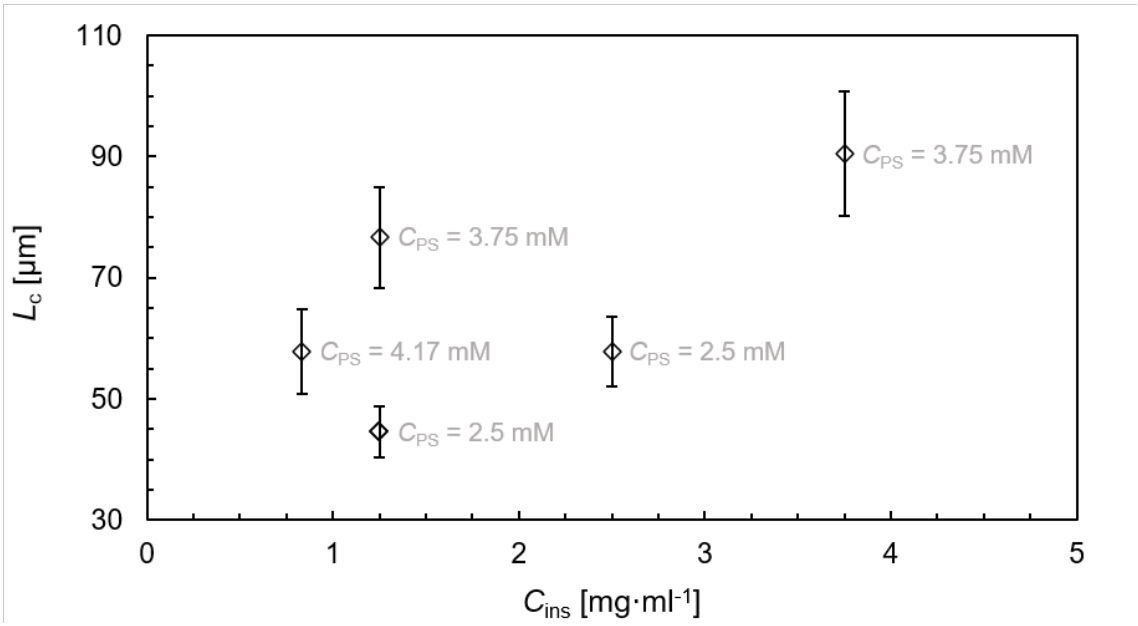

Figure 7. Insulin crystal size (L_c) for the experiments conducted in microdroplets at 20 °C in function of the insulin concentration (C_{ins}) (see Figure 6) [C_{PS} defines the precipitating agent ($ZnCl_2$) solution concentration]. [The bars indicate standard deviations from, at least, three independent experiments].

The formed crystals seem to exhibit a rhombohedral shape (Figure 6). Overall, larger insulin crystals are produced at higher insulin concentrations (Figure 7), and lower precipitating agent ($ZnCl_2$) concentrations seem to induce the formation of agglomerates and/or aggregates [Figure 6-(b)]. A clear formation of aggregates occurs at the lowest precipitating agent solution concentration (1.6 mM), and few aggregates are also observed after 1 day at the second lowest precipitating agent solution concentration, 3.1 mM [and insulin concentration of 1.25 mg·ml^{-1}, Figure 6-(e)]. An opposite behaviour is observed during the hanging-drop experiments as higher insulin concentrations tend to lead to the formation of more agglomerates and/or aggregates (Figures 2 and 4). At lower insulin concentrations, drops from the hanging-drop experiments do not seem to present crystals (*SI – S1. Screening of insulin crystallization conditions*), while at identical insulin concentrations, crystals are produced in the droplet-based microreactor [Figures 6-(a), 6-(d), and 6-(f)]. At an identical precipitating agent concentration, larger

crystals seem to be produced at higher insulin concentrations (Figure 6), but there is not any clear effect on the number of crystals (Figure 7).

Finally, by combining the initial screening of insulin crystallization conditions (Figures 2–5) and the results from the microdroplets experiments (Figures 6 and 7), it is possible to draw an operating regime map to define the insulin and precipitating agent ($ZnCl_2$) solution concentrations (Figure 8).

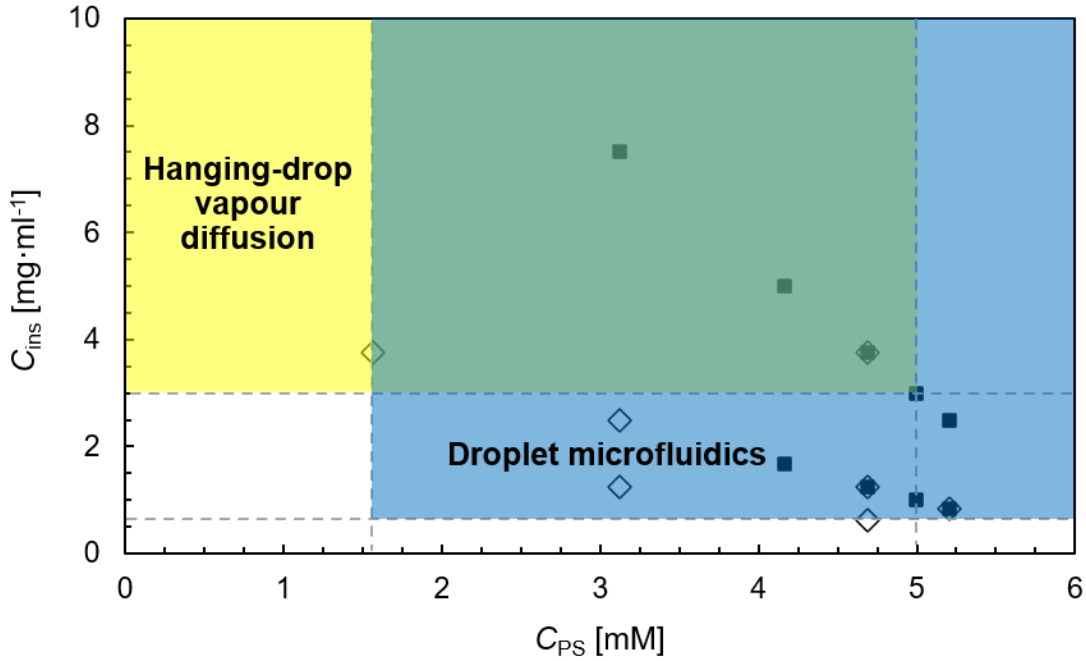

Figure 8. Operating regime map to produce insulin crystals by: (■) hanging-drop vapour diffusion (region highlighted in yellow), and (◊) droplet microfluidics (region highlighted in blue) (20 ºC) experiments [region highlighted in green where crystals are simultaneously generated by both crystallization techniques], which is represented in terms of the precipitating agent ($ZnCl_2$) concentration (C_{PS}) as a function of the insulin concentration (C_{ins}).

It is observed that the formation of insulin crystals requires distinct conditions for the two applied crystallization techniques (Figure 8). The first reason is explained based on the supersaturation level and the rate of supersaturation, which differ depending on the employed crystallization technique [61]. During the hanging-drop assays, the drop

solution undergoes an increase in relative supersaturation due to both increase of the protein and precipitating agent concentrations, which might eventually lead to enter the supersaturated region. Equilibrium is reached when the precipitating agent concentration in the drop is approximately the same as in the reservoir. In microbatch trials, a supersaturated solution is generated right from the beginning as soon as the protein and the precipitating solutions are perfectly mixed. Additionally, the acetone concentration evolution also differs for the two applied crystallization techniques, which has a direct impact on the solubility concentration. Bergeron *et al*. (2003) [3] reported that higher acetone concentrations lead to a higher insulin solubility and, consequently, a lower supersaturation level. However, Hodzhaoglu *et al*. (2016) [32] highlighted that acetone is used to control the nucleation step [32], and the authors concluded that a reduction on insulin solubility occurs in the presence of acetone. Therefore, additional insulin crystallization assays are performed in the absence of acetone. Acetone was substituted by the solvent (HCl) as suggested by Bergeron *et al*. (2003) [3], Reviakine *et al*. (2003) [62], and Hodzhaoglu *et al*. (2016) [32]. The obtained results reveal that no crystals are produced in the absence of acetone (Figure S1, *SI – S2. Insulin crystallization in the absence of acetone*). Due to nuclei formation and subsequent growth, both the supersaturation level and the protein concentration decrease over time. Clear microdroplets (without aggregates) are observed for most of the cases after 1 day (Figure 6), while some of the hanging-drops still exhibit aggregates and/or agglomerates even after 15 days (Figure 3). The second reason is related to the time required to reach homogeneous micromixing. The mixing in the hanging-drop is exclusively governed by liquid diffusion within the drop, which is a very slow process and might differ from drop to drop [63]. This is especially clear during the initial captured time (Figures 2 and 4) (after 4 h). The convection contribution during the droplet generation allows a

homogeneous distribution of the protein and precipitating agent inside the droplet during the microfluidic assays, which might contribute to a narrow CSD (Figures 6 and 7). Lastly, the third reason might be due to interfacial effects. Besides the distinct volumes, the interface nature (gas-liquid *versus* liquid-liquid) also differs and might explain the distinct crystallization outcome (Figures 2, 4, and 6).

Finally, additional experiments are performed at an insulin concentration of 3.75 mg·ml^{-1} for different temperatures (10 °C, 15 °C, and 20 °C) (Figure 9). This protein concentration results in the largest insulin crystal size (90.5 ± 10.2 μm) among the studied concentration range (Figure 7).

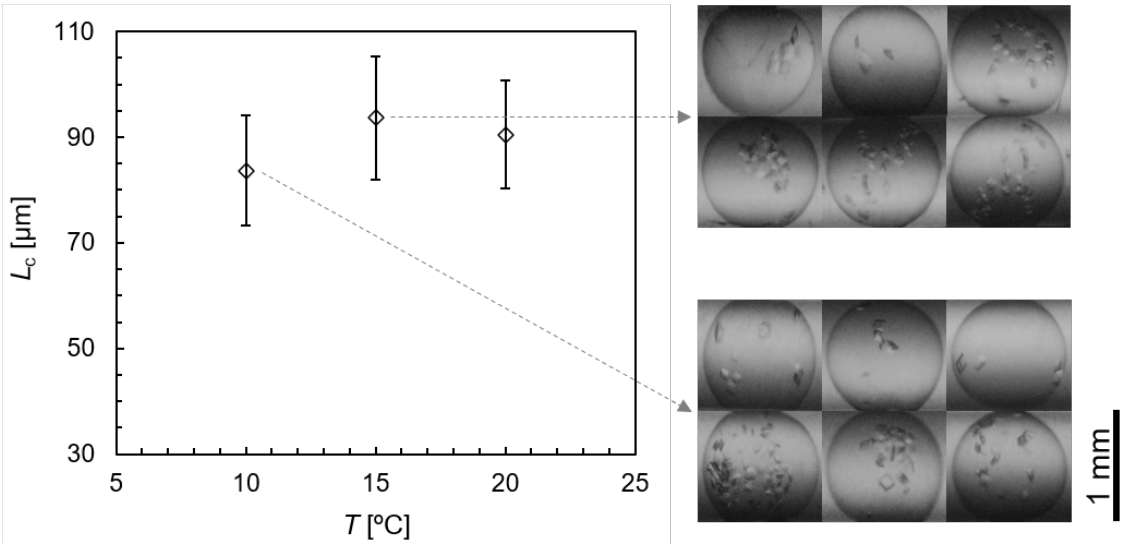

Figure 9. Insulin crystal size (L_c) for the experiments conducted in microdroplets for three different temperature values (T) and a few droplets with crystals collected after 1 day. [The bars are standard deviations from, at least, three independent experiments].

From the current experiments, no clear effect of the temperature on the crystal size for a temperature range from 10 °C to 20 °C is observed (Figure 9). This follows the observations by Nanev *et al*. (2013) [28]. The authors reported identical number density of nucleated insulin crystals at different initial supersaturation values and a temperature

range around 5 °C. In most of the reported works, the CSD is not presented to possibly compare the average crystal size, only a few pictures of the crystals are available. Therefore, with the available pictures from the literature, rhombohedral crystals were measured following a similar procedure compared to the one adopted in the present study (see *2. Methodology and Materials*). The main results including crystal size and crystallization conditions are displayed in Table 1.

Table 1. Insulin crystal size and respective crystallization conditions in different works.

Author(s)	Temperature [ºC]	Insulin concentration [mg·ml^{-1}]	Crystallization time [days]	Crystallizer specifications	Crystal size [μm]
Bergeron *et al.* (2003) [3]	4	0.75–5.0	Several	Glass vials 200 μl	25.4 ± 2.0
Penkova *et al.* (2004) [9]	5–23	2.0	2	Glass capillary 2138 μl	~ 1000
Parambil *et al.* (2011) [34]	10	2.5	2	Glass capillaries (d_c = 2 mm)	300–450
Nanev & Hodzhaoglu (2012) [29]	Nucleation: 4 Growth: 18–29	0.75–5.0	Several	Customized glass cells 350 μl	~ 500
Nanev *et al.* (2013) [28]	Nucleation: 4 Growth: 22–26	5.0	1	Customized glass cells 350 μl	18.0 ± 9.0
	Nucleation: 4 Growth: 20–24	7.0	1		17.6 ± 4.0
Chen *et al.* (2017) [35]	Room temperature	2.0	1	Microwells (w_m = 100 μm)	43.3 ± 2.0
Present study	10	3.75	1	Microdroplets (L_d = 1.3 mm) 1 μl	83.7 ± 10.4
	15				93.7 ± 11.7
	20				90.5 ± 10.2

[**Note**: d_c – capillary diameter, w_m – microwell width, L_d – droplet length.]

The present study as well as the works reported by Bergeron *et al*. (2003) [3], Nanev *et al*. (2013) [28], and Chen *et al*. (2017) [35] observed narrower size distributions in comparison to the remaining cases (Table 1). In particular, Nanev *et al*. (2013) [28] also reported crystal size values after 3 days, where the size roughly triplicates compared to the crystals after a single day of growth time. This might explain the larger crystal size obtained after several days by Penkova *et al*. (2004) [9], Bergeron *et al*. (2003) [3], and Nanev & Hodzhaoglu (2012) [29]. Penkova and co-workers conducted experiments through a supersaturation gradient along a glass capillary, while Nanev & Hodzhaoglu (2012), and Nanev and co-workers performed crystallization assays with distinct nucleation and crystal growth temperatures (Table 1). From the reported data, it seems that for an insulin concentration below 5 $mg \cdot ml^{-1}$, distinct nucleation and growth temperatures induce the formation of larger crystals. However, for the present study (insulin concentration of 3.75 $mg \cdot ml^{-1}$), no significative differences on the crystal size within the studied temperature range are found (Figure 9 and Table 1).

3.3. Secondary structure analysis

Circular dichroism (CD) measurements provide information about conformational changes in proteins [64,65] and the secondary structure present in the bulk solution [66,67]. The acetone concentration evolution differs for the two employed crystallization techniques, hanging-drop and microbatch, which might have an impact on the solubility limit and, consequently, on the supersaturation level. Therefore, far-UV CD spectra of human insulin (20 μM and 200 μM) in the absence and variable acetone concentration are displayed in Figures 10 and 11. Significant amounts of dimers, tetramers, and hexamers are expected at these concentrations. Huus *et al*. (2005) [42] showed that native insulin is completely hexameric down to a concentration of 0.2 mM.

However, the measurements are difficult for insulin concentrations below 1 μM due to noise problems [51].

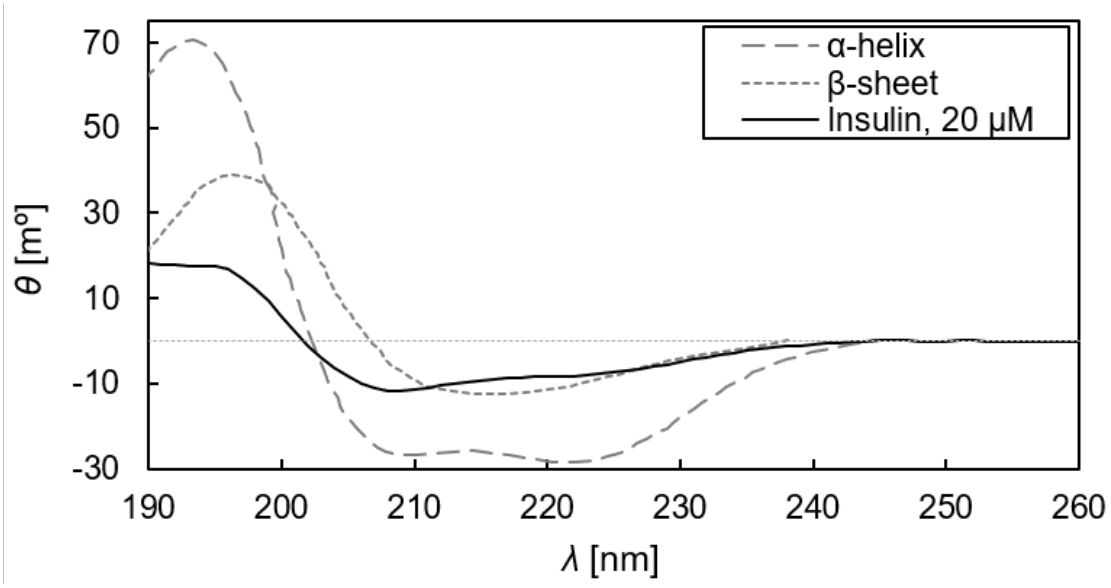

Figure 10. Far-UV spectra of human insulin solution [20 μM, in HCl (20 mM)] and the theoretical spectra (α-helix and β-sheet). Theoretical spectra associated with various types of secondary structure obtained from Kelly *et al*. (2005) [68].

Figure 10 shows the structure of insulin solution in the bulk phase based on its ellipticity (θ) response over the wavelength (λ). This CD spectrum reveals a relatively flat ellipticity response for the measured solution. This is typical of structures rich in β-sheets rather than α-helices [69]. However, the solution exhibits a positive maximum ellipticity around 195 nm, and two negative minima ellipticity at 209 nm and 222 nm (Figure 10). These are typical α-helical characteristics [38,41], which might indicate that the CD spectrum of human insulin in solution corresponds to a mixture of insulin monomers and higher associate states [46,66]. Acidic insulin solutions also have a predominantly native-like α-helical structure [38].

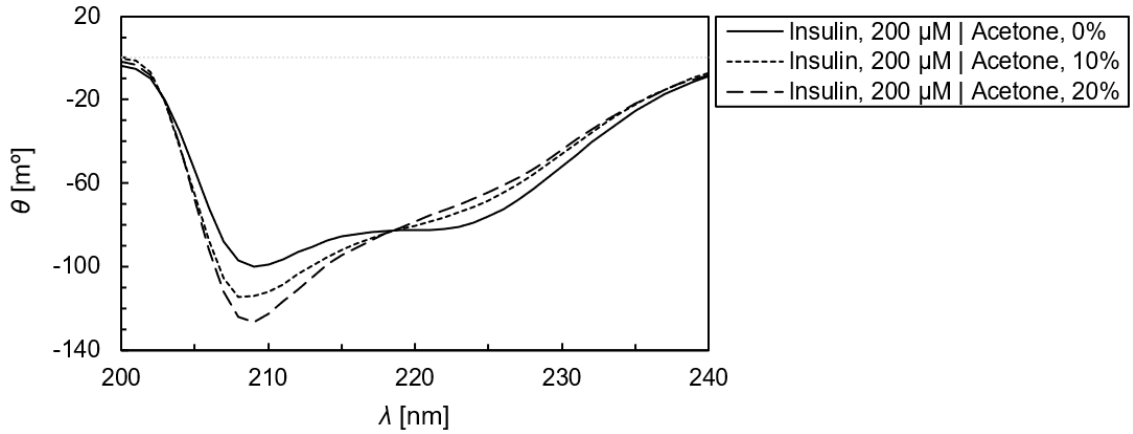

Figure 11. Far-UV spectra of human insulin solutions [200 μM, in HCl (20 mM)] at variable acetone concentrations, and the theoretical spectra (α-helix, β-sheet, and random coil).

The negative minimum ellipticity at 222 nm (Figures 10 and 11) is more evident at higher acetone concentration (Figure 11) [51]. Significant differences can be observed in the far-UV CD spectrum of insulin as a function of acetone concentration as shown in Figure 11. Even though an increase on the peak intensity under the presence of acetone (λ = 209 nm) is observed, the peak is not shifted to lower wavelengths (Figure 11). This scenario may exclude the appearance of structures rich in β-sheets, especially because the presence of extensive β-sheet structures is characterized by a minimum in ellipticity at around 215 nm [38,70]. On the other hand, wavelength shift of the positive maximum ellipticity from λ = 195 nm (acetone-free solutions) to higher wavelengths (insulin-acetone solutions) is observed (Figure 11).

The ratio between the ellipticity at 222 nm and ellipticity at 209 nm indicates whether an isolated helix or several helices that form a coiled-coil are present [40]. Isolated helical states exhibit a ratio value around 0.9, which is the case for the acetone-free solution (Figure 11) at higher insulin concentrations. The solutions with acetone have lower ratio values, and independent of the insulin concentration. As none of the studied cases has a ratio value higher than 1.1, apparently no random coils are formed [64,70,71].

Although the disappearance of the 222 nm-band is observed with the addition of acetone, the minimum peak at 209 nm is not shifted to lower wavelengths (Figure 11). Typically, a random coil structure is characterized by a single minimum below 200 nm [38,70] or very low ellipticity above 210 nm [71]. Finally, the insulin samples (both in presence and absence of acetone) were incubated at 20 ºC and the far-UV CD spectra were compared over time. Even for long times (7 days), no significative differences were obtained. Similarly, Pease *et al*. (2010) [22] concluded that the CD revealed no secondary structural changes in solution, thus no increase of the β-sheet content.

4. Conclusion

This work addresses the production of insulin crystals using two different crystallization techniques, hanging-drop vapour diffusion and droplet microfluidics, and, ultimately, the derivation of an operating regime map. At low protein concentrations, aggregate and/or agglomerate formation is observed during the hanging-drop experiments, while crystals with variable size are produced in the droplet-based microreactor. This distinct behaviour is attributed to three main factors: supersaturation levels reached during the assays, time required to achieve homogeneous micromixing, and interfacial effects. The different supersaturation level might be related to the acetone concentration in solution, which appears to change insulin's secondary structure. Circular dichroism spectra indicate that both α-helix and β-sheet might coexist in the secondary structure of human insulin, but predominantly helical. For the studied conditions, human insulin in solution corresponds to an equilibrium mixture of insulin monomers and higher associate states. At a higher insulin concentration (200 μM), the results highlight the appearance of α-helix structure. Lastly, the addition of acetone exhibits significative

differences, where the main conclusion is the reduction of α-helical content, while excluding the appearance of structures rich in β-sheets or random coils. The presence of acetone is required to generate insulin crystals.

The crystal size presents a high uniformity when produced in the droplet-based microreactor, where the values are within the range reported in the literature. Therefore, this crystallization technique reveals an enhanced control over the crystallization process due to the less occurrence of aggregation and/or agglomeration, and uniform crystal size. Additionally, contrary to what has been reported for other proteins (*e.g.* lysozyme), the temperature effect on crystal size is not observed for insulin in the studied operating conditions. Moreover, droplet microfluidics constitutes a more rational approach to crystallize other proteins (*e.g.* hard-to-crystallize), and brings new perspectives to possibly scale-up the crystallization process or even to perform continuous experimentation.

5. Acknowledgements

S.K. acknowledges funding from the European Research Council under the ERC Starting Grant agreement no. 677169–MicroParticleControl. This work was financially supported by: Base Funding - UIDB/00511/2020 of the Laboratory for Process Engineering, Environment, Biotechnology and Energy – LEPABE – funded by national funds through the FCT/MCTES (PIDDAC).

6. References

[1] D. Crowfoot, X-Ray Single Crystal Photographs of Insulin, Nature. (1935) 591–592.

[2] J.A.K. Howard, Dorothy Hodgkin and her contributions to biochemistry, Nature Reviews Molecular Cell Biology. 4 (2003) 891–896. https://doi.org/10.1038/nrm1243.

[3] L. Bergeron, L.F. Filobelo, O. Galkin, P.G. Vekilov, Thermodynamics of the Hydrophobicity in Crystallization of Insulin, Biophysical Journal. 85 (2003) 3935–3942. https://doi.org/10.1016/S0006-3495(03)74807-3.

[4] J. Brange, Galenics of Insulin: The Physico-chemical and Pharmaceutical Aspects of Insulin and Insulin Preparations, 1st Edition, Springer-Verlag Berlin Heidelberg, Berlin, 1987.

[5] H.P. Merkle, A. Jen, A crystal clear solution for insulin delivery, Nature Biotechnology. 20 (2002) 789–790. https://doi.org/10.1038/nbt0802-789.

[6] M. Norrman, G. Schluckebier, Crystallographic characterization of two novel crystal forms of human insulin induced by chaotropic agents and a shift in pH, BMC Structural Biology. 7 (2007) 1–14. https://doi.org/10.1186/1472-6807-7-83.

[7] C.N. Nanev, F. V. Hodzhaoglu, I.L. Dimitrov, Kinetics of insulin crystal nucleation, energy barrier, and nucleus size, Crystal Growth & Design. 11 (2011) 196–202. https://doi.org/10.1021/cg1011499.

[8] E.K. Lee, W. Kim, Isolation and Purification of Proteins, 1st Edition, CRC Press, 2003.

[9] A. Penkova, I. Dimitrov, C. Nanev, Nucleation of insulin crystals in a wide continuous supersaturation gradient, Annals of the New York Academy of Sciences. 1027 (2004) 56–63. https://doi.org/10.1196/annals.1324.006.

[10] J.J. Abel, Crystalline Insulin, PNAS. 10 (1926) 132–136. https://doi.org/10.7326/0003-4819-10-9-1335.

[11] J. Schlichtkrull, R. Ekholm, A. Norman, B. Noer, L. Reio, Insulin Crystals. III. Determination of the Rhombohedral Zinc-Insulin Unit-Cell by Combined Microscopical and Chemical Examinations., Acta Chemica Scandinavica. 11 (1957) 291–298. https://doi.org/10.3891/acta.chem.scand.11-0291.

[12] J. Schlichtkrull, R. Ekholm, A. Norman, B. Noer, L. Reio, Insulin Crystals. IV. The Preparation of Nuclei, Seeds, and Monodisperse Insulin Crystal Suspensions., Acta Chemica Scandinavica. 11 (1957) 299–302. https://doi.org/10.3891/acta.chem.scand.11-0299.

[13] J. Schlichtkrull, R. Ekholm, A. Norman, B. Noer, L. Reio, Insulin Crystals. V. The Nucleation and Growth of Insulin Crystals., Acta Chemica Scandinavica. 11 (1957) 439–460. https://doi.org/10.3891/acta.chem.scand.11-0439.

[14] J. Schlichtkrull, R. Ekholm, A. Norman, B. Noer, L. Reio, Insulin Crystals. VI. The Anisotropic Growth of Insulin Crystals., Acta Chemica Scandinavica. 11

(1957) 484–486. https://doi.org/10.3891/acta.chem.scand.11-0484.

[15] J. Schlichtkrull, R. Ekholm, A. Norman, B. Noer, L. Reio, Insulin Crystals. VII. The Growth of Insulin Crystals., Acta Chemica Scandinavica. 11 (1957) 1248–1256. https://doi.org/10.3891/acta.chem.scand.11-1248.

[16] W. Kadima, A. McPherson, M.F. Dunn, F. Jurnak, Precrystallization aggregation of insulin by dynamic light scattering and comparison with canavalin, Journal of Crystal Growth. 110 (1991) 188–194. https://doi.org/10.1016/0022-0248(91)90884-8.

[17] C.M. Yip, M.D. Ward, Atomic force microscopy of insulin single crystals: Direct visualization of molecules and crystal growth, Biophysical Journal. 71 (1996) 1071–1078. https://doi.org/10.1016/S0006-3495(96)79307-4.

[18] E.J. Nettleton, P. Tito, M. Sunde, M. Bouchard, C.M. Dobson, C. V. Robinson, Characterization of the oligomeric states of insulin in self-assembly and amyloid fibril formation by mass spectrometry, Biophysical Journal. 79 (2000) 1053–1065. https://doi.org/10.1016/S0006-3495(00)76359-4.

[19] P. Mühlig, T. Klupsch, U. Schell, R. Hilgenfeld, Observation of the early stage of insulin crystallization by confocal laser scanning microscopy, Journal of Crystal Growth. 232 (2001) 93–101. https://doi.org/10.1016/S0022-0248(01)01070-3.

[20] L. Bromberg, J. Rashba-Step, T. Scott, Insulin particle formation in supersaturated aqueous solutions of poly(ethylene glycol), Biophysical Journal. 89 (2005) 3424–3433. https://doi.org/10.1529/biophysj.105.062802.

[21] C. Govardhan, N. Khalaf, C.W. Jung, B. Simeone, A. Higbie, S. Qu, L. Chemmalil, S. Pechenov, S.K. Basu, A.L. Margolin, Novel long-acting crystal formulation of human growth hormone, Pharmaceutical Research. 22 (2005) 1461–1470. https://doi.org/10.1007/s11095-005-6021-x.

[22] L.F. Pease, M. Sorci, S. Guha, D.H. Tsai, M.R. Zachariah, M.J. Tarlov, G. Belfort, Probing the nucleus model for oligomer formation during insulin amyloid fibrillogenesis, Biophysical Journal. 99 (2010) 3979–3985. https://doi.org/10.1016/j.bpj.2010.10.010.

[23] E. Chatani, R. Inoue, H. Imamura, M. Sugiyama, M. Kato, M. Yamamoto, K. Nishida, T. Kanaya, Early aggregation preceding the nucleation of insulin amyloid fibrils as monitored by small angle X-ray scattering, Scientific Reports. 5 (2015) 1–14. https://doi.org/10.1038/srep15485.

[24] S. Fili, A. Valmas, M. Norrman, G. Schluckebier, D. Beckers, T. Degen, J. Wright, A. Fitch, F. Gozzo, A.E. Giannopoulou, F. Karavassili, I. Margiolaki, Human insulin polymorphism upon ligand binding and pH variation: The case of 4-ethylresorcinol, IUCrJ. 2 (2015) 534–544. https://doi.org/10.1107/S2052252515013159.

[25] S. Dolui, A. Roy, U. Pal, A. Saha, N.C. Maiti, Structural Insight of Amyloidogenic Intermediates of Human Insulin, ACS Omega. 3 (2018) 2452–2462. https://doi.org/10.1021/acsomega.7b01776.

[26] D.A. Barlow, Theory of the intermediate stage of crystal growth with applications to insulin crystallization, Journal of Crystal Growth. 470 (2017) 8–14.

https://doi.org/10.1016/j.jcrysgro.2017.03.053.

[27] D. V. Alexandrov, I.G. Nizovtseva, On the theory of crystal growth in metastable systems with biomedical applications: protein and insulin crystallization, Philosophical Transactions A. 377 (2019) 1–15. https://doi.org/10.1098/rsta.2018.0209.

[28] C.N. Nanev, V.D. Tonchev, F. V. Hodzhaoglu, Protocol for growing insulin crystals of uniform size, Journal of Crystal Growth. 375 (2013) 10–15. https://doi.org/10.1016/j.jcrysgro.2013.04.010.

[29] C.N. Nanev, F. V. Hodzhaoglu, Temperature control of protein crystal nucleation, Crystal Research & Technology. 47 (2012) 1195–1200. https://doi.org/10.1002/crat.201200340.

[30] C.N. Nanev, K.P. Petrov, Steering a crystallization process to reduce crystal polydispersity; case study of insulin crystallization, Journal of Crystal Growth. 480 (2017) 164–169. https://doi.org/10.1016/j.jcrysgro.2016.11.068.

[31] I. Dimitrov, F. Hodzhaoglu, I. Ivanov, In Vitro Dissolution of Insulin Crystal Polymorphs at Model Conditions Relevant to In Vivo Environment, Dissolution Techniques. (2013) 11–16.

[32] F. V Hodzhaoglu, M. Conejero-Muriel, I.L. Dimitrov, J.A. Gavira, Optimization of the classical method for nucleation and growth of rhombohedral insulin crystals by pH titration and screening, Bulgarian Chemical Comunications. 48 (2016) 29–37.

[33] M. Maeda, T. Chatake, I. Tanaka, A. Ostermann, N. Niimura, Crystallization of a large single crystal of cubic insulin for neutron protein crystallography, Journal of Synchrotron Radiation. 11 (2004) 41–44. https://doi.org/10.1107/S0909049503023859.

[34] J. V. Parambil, M. Schaepertoens, D.R. Williams, J.Y.Y. Heng, Effects of Oscillatory Flow on the Nucleation and Crystallization of Insulin, Crystal Growth & Design. 11 (2011) 4353–4359.

[35] F. Chen, G. Du, D. Yin, R. Yin, H. Zhang, W. Zhang, S.-M. Yang, Crystallization of bovine insulin on a flow-free droplet-based platform, AIP Conference Proceedings. 1820 (2017) 1–4. https://doi.org/10.1063/1.4977260.

[36] Y. Li, M. Kvetny, M. Bowen, W. Brown, D. Wang, G. Wang, Method to Directly Measure and Actively Control a Single Nucleation-Crystal Growth Process, Crystal Growth & Design. 19 (2019) 2470–2475. https://doi.org/10.1021/acs.cgd.9b00151.

[37] R. Contreras-Montoya, M. Arredondo-Amador, G. Escolano-Casado, M.C. Mañas-Torres, M. González, M. Conejero-Muriel, V. Bhatia, J.J. Díaz-Mochón, O. Martínez-Augustin, F. Sánchez de Medina, M.T. Lopez-Lopez, F. Conejero-Lara, J.A. Gavira, L. Álvarez De Cienfuegos, Insulin Crystals Grown in Short-Peptide Supramolecular Hydrogels Show Enhanced Thermal Stability and Slower Release Profile, ACS Applied Materials and Interfaces. (2021). https://doi.org/10.1021/acsami.1c00639.

[38] M. Bouchard, J. Zurdo, E.J. Nettleton, C.M. Dobson, C. V. Robinson, Formation of insulin amyloid fibrils followed by FTIR simultaneously with CD and electron microscopy, Protein Science. 9 (2000) 1960–1967. https://doi.org/10.1110/ps.9.10.1960.

[39] S.P. Wood, T.L. Blundell, A. Wollmer, N.R. Lazarus, R.W.J. Neville, The Relation of Conformation and Association of Insulin to Receptor Binding; X-Ray and Circular-Dichroism Studies on Bovine and Hystricomorph Insulins, European Journal of Biochemistry. 55 (1975) 531–542. https://doi.org/10.1111/j.1432-1033.1975.tb02190.x.

[40] D. Bernson, A. Mecinovic, M.T. Abed, F. Limé, P. Jageland, M. Palmlöf, E.K. Esbjörner, Amyloid formation of bovine insulin is retarded in moderately acidic pH and by addition of short-chain alcohols, European Biophysics Journal. 49 (2020) 145–153. https://doi.org/10.1007/s00249-019-01420-0.

[41] E. Kachooei, A.A. Moosavi-Movahedi, F. Khodagholi, H. Ramshini, F. Shaerzadeh, N. Sheibani, Oligomeric forms of insulin amyloid aggregation disrupt outgrowth and complexity of neuron-like PC12 cells, PLoS ONE. 7 (2012) 1–9. https://doi.org/10.1371/journal.pone.0041344.

[42] K. Huus, S. Havelund, H.B. Olsen, M. Van De Weert, S. Frokjaer, Thermal dissociation and unfolding of insulin, Biochemistry. 44 (2005) 11171–11177. https://doi.org/10.1021/bi0507940.

[43] E.H. Strickland, D. Mercola, Near-Ultraviolet Tyrosyl Circular Dichroism of Pig Insulin Monomers, Dimers, and Hexamers. Dipole-Dipole Coupling Calculations in the Monopole Approximation, Biochemistry. 15 (1976) 3875–3884.

[44] S.G. Melberg, W.C. Johnson, Changes in secondary structure follow the dissociation of human insulin hexamers: A circular dichroism study, Proteins: Structure, Function, and Bioinformatics. 8 (1990) 280–286. https://doi.org/10.1002/prot.340080309.

[45] J.W.S. Morris, D.A. Mercola, E.R. Arquilla, An analysis of the near ultraviolet circular dichroism of insulin, BBA - Protein Structure. 160 (1968) 145–150. https://doi.org/10.1016/0005-2795(68)90080-9.

[46] A. Ahmad, V.N. Uversky, D. Hong, A.L. Fink, Early in the fibrillation of monomeric insulin, Journal of Biological Chemistry. 280 (2005) 42669–42675. https://doi.org/10.1074/jbc.M504298200.

[47] L. Nielsen, R. Khurana, A. Coats, S. Frokjaer, J. Brange, S. Vyas, V.N. Uversky, A.L. Fink, Effect of environmental factors on the kinetics of insulin fibril formation: Elucidation of the molecular mechanism, Biochemistry. 40 (2001) 6036–6046. https://doi.org/10.1021/bi002555c.

[48] V.N. Uversky, L.N. Garriques, I.S. Millett, S. Frokjaer, J. Brange, S. Doniach, A.L. Fink, Prediction of the association state of insulin using spectral parameters, Journal of Pharmaceutical Sciences. 92 (2003) 847–858. https://doi.org/10.1002/jps.10355.

[49] D.N. Brems, P.L. Brown, L.A. Heckenlaible, B.H. Frank, Equilibrium

Denaturation of Insulin and Proinsulin, Biochemistry. 29 (1990) 9289–9293. https://doi.org/10.1021/bi00491a026.

[50] M.J. Ettinger, S.N. Timasheff, Optical Activity of Insulin. I. On the Nature of the Circular Dichroism Bands, Biochemistry. 10 (1965) 824–831.

[51] Y. Pocker, S.B. Biswas, Conformational Dynamics of Insulin in Solution. Circular Dichroic Studies, Biochemistry. 19 (1980) 5043–5049. https://doi.org/10.1021/bi00563a017.

[52] J. Goldman, F.H. Carpenter, Zinc Binding, Circular Dichroism, and Equilibrium Sedimentation Studies on Insulin (Bovine) and Several of Its Derivatives, Biochemistry. 13 (1974) 4566–4574. https://doi.org/10.1021/bi00719a015.

[53] J. Ferreira, F. Castro, F. Rocha, S. Kuhn, Protein crystallization in a droplet-based microfluidic device: Hydrodynamic analysis and study of the phase behaviour, Chemical Engineering Science. 191 (2018) 232–244.

[54] J. Ferreira, F. Castro, S. Kuhn, F. Rocha, Controlled protein crystal nucleation in microreactors: The effect of the droplet volume versus high supersaturation ratios, CrystEngComm. 22 (2020) 4692–4701. https://doi.org/10.1039/d0ce00517g.

[55] N.I.E. B.V., NIS-Elements Imaging Software, Nikon Instruments. (2019). www.microscope.healthcare.nikon.com/en_EU/products/software/nis-elements/nis-elements-advanced-research (accessed November 1, 2019).

[56] J. Ferreira, F. Castro, F. Rocha, S. Kuhn, Protein crystallization in a droplet-based microfluidic device: Hydrodynamic analysis and study of the phase behaviour, Chemical Engineering Science. 191 (2018) 232–244. https://doi.org/10.1016/j.ces.2018.06.066.

[57] J. Ferreira, F. Castro, S. Kuhn, F. Rocha, Controlled protein crystal nucleation in microreactors: The effect of the droplet volume: Versus high supersaturation ratios, CrystEngComm. 22 (2020) 4692–4701. https://doi.org/10.1039/d0ce00517g.

[58] P. Zhu, L. Wang, Passive and active droplet generation with microfluidics: a review, Lab on a Chip. 17 (2017) 34–75. https://doi.org/10.1039/C6LC01018K.

[59] ImageJ, ImageJ, (2019). imagej.net/ImageJ (accessed November 15, 2019).

[60] A. Sauter, F. Roosen-Runge, F. Zhang, G. Lotze, R.M.J. Jacobs, F. Schreiber, Real-time observation of nonclassical protein crystallization kinetics, Journal of the American Chemical Society. 137 (2015) 1485–1491. https://doi.org/10.1021/ja510533x.

[61] J.A. Gavira, Current trends in protein crystallization, Archives of Biochemistry and Biophysics. 602 (2016) 3–11. https://doi.org/10.1016/j.abb.2015.12.010.

[62] I. Reviakine, D.K. Georgiou, P.G. Vekilov, Capillarity effects on crystallization kinetics: Insulin, Journal of the American Chemical Society. 125 (2003) 11684–11693. https://doi.org/10.1021/ja030194t.

[63] P.M. Martins, J. Pessoa, Z. Sárkány, F. Rocha, A.M. Damas, Rationalizing Protein Crystallization Screenings through Water Equilibration Theory and Protein Solubility Data, Crystal Growth & Design. 8 (2008) 4233–4243.

[64] S. Kelly, N. Price, The Use of Circular Dichroism in the Investigation of Protein Structure and Function, Current Protein & Peptide Science. 1 (2005) 349–384. https://doi.org/10.2174/1389203003381315.

[65] S.M. Kelly, T.J. Jess, N.C. Price, How to study proteins by circular dichroism, Biochimica et Biophysica Acta - Proteins and Proteomics. 1751 (2005) 119–139. https://doi.org/10.1016/j.bbapap.2005.06.005.

[66] S.H. Mollmann, L. Jorgensen, J.T. Bukrinsky, U. Elofsson, W. Norde, S. Frokjaer, Interfacial adsorption of insulin: Conformational changes and reversibility of adsorption, European Journal of Pharmaceutical Sciences. 27 (2006) 194–204. https://doi.org/10.1016/j.ejps.2005.09.010.

[67] R. Docherty, Engineering Crystallography: From Molecule to Crystal to Functional Form, Springer, Erice, Sicily, Italy, 2017. https://doi.org/10.1007/978-94-024-1117-1.

[68] S.M. Kelly, T.J. Jess, N.C. Price, How to study proteins by circular dichroism, Biochimica & Biophysica Acta. 1751 (2005) 119–139. https://doi.org/10.1016/j.bbapap.2005.06.005.

[69] V.S. Balaraj, P.C.H. Zeng, S.P. Sanford, S.A. McBride, A. Raghunandan, J.M. Lopez, A.H. Hirsa, Surface shear viscosity as a macroscopic probe of amyloid fibril formation at a fluid interface, Soft Matter. 13 (2017) 1780–1787. https://doi.org/10.1039/c6sm01831a.

[70] D.M. Rogers, S.B. Jasim, N.T. Dyer, F. Auvray, M. Réfrégiers, J.D. Hirst, Electronic Circular Dichroism Spectroscopy of Proteins, Chem. 5 (2019) 2751–2774. https://doi.org/10.1016/j.chempr.2019.07.008.

[71] N.J. Greenfield, Using circular dichroism spectra to estimate protein secondary structure, Nature Protocols. 1 (2007) 2876–2890. https://doi.org/10.1038/nprot.2006.202.